Magnetic Fields and the Crystallization of White Dwarfs

Jordi Isern,[1,2] Enrique García-Berro,[3,2] Baybars Külebi,[2] and Pablo Lorén-Aguilar[4]

[1]*Institut de Ciències de l'Espai (ICE-CSIC), Campus UAB Bellaterra, Barcelona, Spain;* `isern@ice.cat`

[2]*Institut d'Estudis Espacials de Catalunya (IEEC), Barcelona, Spain;* `bkulebi@gmail.com`

[3]*Universitat Politècnica de Catalunya (UPC), Barcelona, Spain;* `Enrique.Garcia-Berro@upc.edu`

[4]*School of Physics and Astronomy, University of Exeter, Exeter, United Kingdom;* `pablo@astro.ex.ac.uk`

Abstract. The evolution of white dwarfs can be described as a cooling process. When the temperature is low enough, the interior experiences a phase transition and crystallizes. Crystallization introduces two new sources of energy, latent heat and chemical sedimentation, and induces the formation of a convective mantle around the solid core. This structure, which is analogous to that of the Earth, could induce the formation of a magnetic field via dynamo mechanism. In this work we discuss the viability of such mechanism, and its use as a diagnostic tool of crystallization.

1. Introduction

The interior of the majority of single white dwarf stars is made of a completely ionized mixture of ^{12}C and ^{16}O plus some impurities, like ^{22}Ne and ^{56}Fe. The thermodynamic properties of nuclei can be described by the equation of state of a Coulomb plasma while those of electrons by that of an ideal Fermi gas. Because of electron degeneracy, the evolution of such stars is just a gravothermal process of cooling where nuclear reactions only play a secondary role if any, see Althaus et al. (2010) for a recent review.

During the cooling process, the plasma experiences a phase transition and crystallizes into a classical body-centered cubic crystal (bcc), the detailed structure being rather uncertain since the free energy of the different Coulomb crystals is very similar at low temperatures. In the case of one component plasma with atomic number Z, this occurs when the Coulomb parameter $\Gamma = Z^2e^2/ak_BT$, where $a = [3/(4\pi n_i)]^{1/3}$ is the ion-sphere radius, n_i is the ion number density and k_B is the Boltzmann constant, becomes larger then ~ 175. Solidification introduces two additional sources of energy in the cooling process, latent heat and gravitational sedimentation. The importance of the latent heat was early recognized (Van Horn 1988; Shaviv & Kovetz 1976), but that of sedimentation has taken more time.
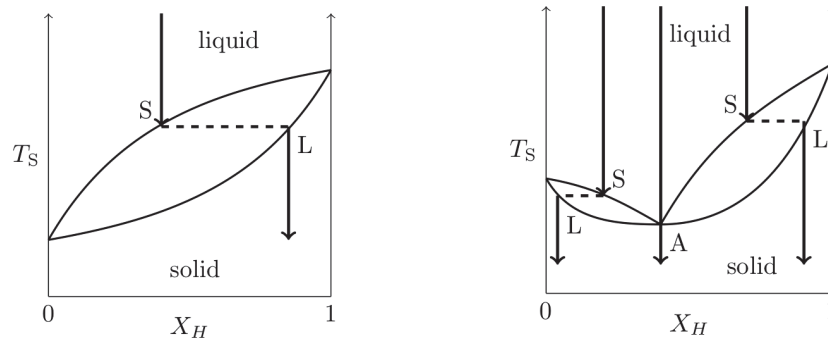
Figure 1.   Phase diagrams of a Coulomb binary mixture. The left panel represents the spindle case and the right panel represents the azeotropic case. Labels L show the point where the solid liquifies and labels S where the liquid solidifies. Point A is the azeotropic point.

The first to realize that Coulomb plasmas could experience a change of miscibility during the process of solidification was Schatzman (1958), but it has been necessary to wait for the detailed calculations of phase diagrams to explore the consequences of such an effect. The first phase diagram of the two dominant chemical species, ^{12}C and ^{16}O, was obtained by Stevenson (1980) who found an eutectic behavior with a complete separation of both species upon crystallization. These calculations were improved by Ichimaru et al. (1988); Barrat et al. (1988); Ogata et al. (1993) and Segretain & Chabrier (1993) (SC hereafter) who found a phase diagram of the spindle form (Fig. 1). This phase diagram was recently reexamined by Horowitz et al. (2010) who found an azeotropic behavior (Fig. 1) and a noticeably lower temperature of crystallization as compared with the SC diagram. If the phase diagram has a spindle form the solid formed upon crystallization is richer in oxygen and denser than the liquid. Consequently, the solid settles down and the liquid excess of carbon that is left behind is redistributed by Rayleigh-Taylor instabilities. The result is an enrichment of oxygen in the central layers and its depletion in the outer ones, with the subsequent release of gravitational energy (Schatzman 1982; Mochkovitch 1983; Segretain et al. 1994; Isern et al. 1997, 2000).

The sedimentation of minor species is intricate since it depends on the behaviour of a multicomponent phase diagram that is not well known. The most abundant impurity in white dwarfs is ^{22}Ne, with an abundance directly related to the initial abundances of CNO elements which, after the hydrogen and helium-burning phases are converted to ^{22}Ne. Because of its high neutron number and the high sensitivity of degenerate structures to the electron number profile, the migration of ^{22}Ne to the inner layers can induce a large release of gravitational energy (Isern et al. 1991). A similar effect can be produced by the deposition of ^{56}Fe at the centre (Xu & Van Horn 1992). Within the hypothesis of an effective binary mixture, the phase diagram displays an azeotropic behavior (Fig. 1) in the case of ^{22}Ne and a eutectic behaviour in the case of ^{56}Fe (Segretain et al. 1994). In both cases, the abundances of the impurities are smaller than the azeotropic or eutectic values and the solid in equilibrium with the liquid has a smaller concentration of impurities. Being lighter, it rises and melts at lower density regions where it mixes via Rayleigh-Taylor instabilities. Meanwhile, the concentration of impurities in the liquid increases until it reaches the azeotropic or the eutectic values
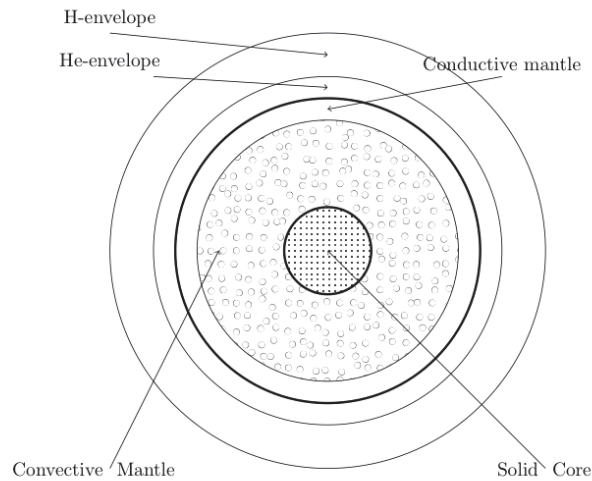
Figure 2.   Structure of a crystallizing CO white dwarf star.

respectively and freezes. This process of distillation continues until all the impurity is trapped in a central region with an abundance that depends on the detailed properties of the phase diagram (Schatzman 1982; Mochkovitch 1983).

Despite that more than 30 years have elapsed since the phase diagrams were computed for the first time, no direct proof has been provided that a sedimentation induced by a phase transition really occurs in the interior of solidifying white dwarfs. The only indirect evidence has been provided by the discrepancy in the age of NGC 6791 obtained from the age of the main sequence stars and white dwarfs (8 and 6 Gyr, respectively) that disappears when diffusion and sedimentation are included in the calculations (Garcia-Berro et al. 2010).

It is well known that rotating planets and stars can develop magnetic fields if they have convective zones in their interior. As already noted, in the case of white dwarfs the sedimentation induced by crystallization leads to the formation of a solid core that grows with time, surrounded by an almost isothermal liquid mantle that is rehomogenized by convective motions driven by Rayleigh-Taylor instabilities (Fig. 2). This situation is similar to that found in the Earth and Jupiter, and it is natural to wonder if these convective motions are able to generate a magnetic field strong enough to be used as a diagnostic tool of the sedimentation process in the case of white dwarfs.

2. Models and Results

The total amount of energy released by the sedimentation induced by crystallization is 2×10^{46} erg if the SC phase diagram is used and the white dwarf is made of half carbon and half oxygen. The energy released by the sedimentation of impurities is in the range of $2 \times 10^{45} - 1.5 \times 10^{47}$ in the case of ^{22}Ne ($X_{22} = 0.02$) and 2×10^{46} in the case of ^{56}Fe ($X_{56} = 0.001$), again in cgs units. The importance of impurities is a consequence of the extreme sensitivity of electron degenerate structures to the number of electrons per nucleon.

The energy release in the convective mantle depends on the initial mass and metallicity of the parent star, which determines the radial profile of the carbon and oxygen and of the distribution of impurities (Isern et al. 1997, 2000). The rate of solidification is limited by the luminosity of the star which, in turn, depends on the temperature of the core, the mass of the white dwarf and the nature of the partially or non-degenerate envelope. DA white dwarfs, that represent ~ 80 % of the total, are characterized by the presence of hydrogen in their photosphere and the envelope is made of two layers of almost pure helium and hydrogen respectively, being the He layer the most internal one. The mass of the helium layer is $\sim 10^{-2} M_{\mathrm{WD}}$, while the mass of the hydrogen layer can have different values but is always smaller than $\sim 10^{-4} M_{\mathrm{WD}}$. Non-DA white dwarfs are characterized by the absence of hydrogen in their photosphere and, consequently are more luminous for the same temperature of the core. Typical values of ε_{g} found from the beginning to the end of the crystallization process are in the range of (Isern et al. 1997, 2000) 1.2×10^{13} and 2.5×10^{12} erg/g, and from 6×10^{13} and 1.2×10^{12} for a 0.61 and 1.00 $M_{\odot}$ respectively, in the case of CO separation and using the BaSTI profiles (Salaris et al. 2010).

Solidification starts at $\log L/L_{\odot} = -2.6$ and -3.6 for the two cases mentioned before, while the central temperatures and densities are $\log T_{\mathrm{c}} = 6.6$ and 6.3 and $\log \rho_{\mathrm{c}} = 7.5$ and 6.6 respectively (in cgs units). These values correspond to a strongly degenerate Coulomb plasma which typically has small viscosities and large thermal and electrical conductivities (Nandkumar & Pethick 1984). If, for simplicity, we limit ourselves to the case of a 1 $M_{\odot}$ star, the difference of density between the pure carbon bubbles and the ambient liquid mixture is $\delta\rho/\rho \sim 10^{-3}$ which means that for a typical effective acceleration $a_{\mathrm{eff}} = g(\delta\rho/\rho)$ of 1.8×10^6 cm^2 s^{-1} and a mixing length of 2×10^8 cm the carbon bubbles can reach velocities of ~ 300 km/s. However, if drag forces are taken into account, these velocities are reduced by an order of magnitude. This plasma has an electrical conductivity $\sigma = 1.3 \times 10^{21}$ s^{-1}, a magnetic diffusivity $\eta = 5.6 \times 10^{-2}$ cm^2 s^{-1} and a kinematic viscosity 3.13×10^{-2} cm^2 s^{-1}. Consequently the magnetic Prandtl number is Pm ≈ 0.58 and the Reynolds and magnetic Reynolds numbers are very large, $\sim 10^{17}$. Furthermore, the characteristic ohmic decay time, $\tau_{\mathrm{ohm}} \sim L^2/\eta$ is $\sim 10^{18}$ s, much larger than the age of the white dwarf, which means that once created the magnetic field will remain almost constant during time.

The aim of the dynamo scaling theories is to explain the properties of magnetic fields in terms of the fundamental properties of the region hosting the dynamo in order to obtain basic information about the planet or star under study. Many of these theories relay on the balance between the Coriolis and the Lorentz forces while some others rely on the balance between the ohmic dissipation and the energy flux available to the dynamo (Christensen 2010). This scaling law can be extended to fully convective stars like T Tauri and rapidly rotating M dwarfs (Christensen et al. 2009), and it is natural, given the similarity between the internal convective zone of white dwarfs and the interior of Earth an Jupiter, to apply it to crystallizing white dwarfs.

If it is assumed that the ohmic dissipation scales with the magnetic Reynolds number and that convection is described with the mixing length formalism, this scaling law predicts that the strength of the magnetic field will be (Christensen 2010):

$$\frac{B^2}{2\mu_0} = cf_{\Omega}\frac{1}{V} \int_{r_i}^{r_s} \left[\frac{q_c(r)L(r)}{H(r)}\right]\rho(r)^{1/3} 4\pi r^2 dr \tag{1}$$

where V is the volume of the convective zone, r_s and r_i are the outer and the inner radius of the convective shell, L is the mixing length (the minimum between the density scale height and the width of the convective zone, $r_s - r_i$). Here it has been assumed that $L = H$ and $f_\Omega = 1$, and the integral has been performed using the BaSTI models of white dwarfs.

The dynamo starts when solidification begins, it reaches a maximum and then slowly declines as the bottom of the convective mantle moves outwards and the star fades. The density of energy available to the dynamo depends on the mass of the star, which determines the intensity of the gravitational field, and the luminosity of the star, that determines the rate at which the star crystallizes. This luminosity, in turn, depends on the transparency of the atmosphere and temperature of the core. The maximum energy available to the dynamo ranges from $\log E_{dyn}(\text{ergs cm}^{-3}) = 8.2$ to 9.6 and from 8.3 to 9.7 for DA and non-DA stars, respectively, when the mass varies from 0.54 to $1.0\, M_\odot$. The scaling law that links the magnetic fields of Earth, Jupiter, T Tauri and M dwarf stars can be approximated by $\log B = 0.5 \log E_{dyn} - 5.42$ (again in cgs units) and predicts, at the top of the dynamo, a magnetic field with a maximum intensity in the range $\sim 0.05 - 0.25$ MG for a wide dwarf mass range of $0.54 - 1.0\, M_\odot$, respectively. Models suggest that the field would be smaller at the surface (Christensen et al. 2009).

The distribution of observed intensities of isolated magnetic white dwarfs seems to have a bimodal structure. There is a group with magnetic fields in the range of $1 - 1,000$ MG and another with intensities $\lesssim 0.1$ MG and almost no star has magnetic fields $0.1 - 1$ MG (Ferrario et al. 2015). It is tempting to attribute the existence of this group of stars with a relatively small magnetic field to the crystallization process. If this were the case, it would be expected that all white dwarfs would see its inherited magnetic field enhanced when crossing the solidification line. The intensity of the resulting field would depend on the properties of each white dwarf, mainly the rotation rate, as it is the case of red dwarfs (Christensen et al. 2009). In any case, cool white dwarfs with a solid core should display larger magnetic fields that hotter ones.

Two arguments in favor of such hypothesis can be advanced. First, Ferrario et al. (2015) showed that, in general, there is no correlation between the intensity of the magnetic field and the effective temperature of the star, which is in agreement with the fact that these magnetic fields have a very long lifetime. However, when we restrict ourselves to the low intensity sample, objects with fields $\lesssim 50$ kG seem to be hotter than objects with fields $\gtrsim 50$ kG. Nevertheless, as noted by Ferrario et al. (2015), this could be a consequence of several selection effects, so this point demands a better sample in order to provide a definite answer. The second argument comes from the so-called high $\log g$ problem (Tremblay et al. 2011; Kepler et al. 2013), which consists in the fact that the average mass of white dwarfs with $T_{eff} \lesssim 13,000$ K is larger than that of stars hotter than this value. A natural explanation would be the presence of an undetected magnetic field that is adding a Zeeman splitting to the natural gravity broadening of the Balmer lines.

3.   Conclusions

As a consequence of phase transitions there is a strong migration of chemical elements in the interior of white dwarfs. The analogy with the terrestrial geodynamo suggests that these convective motions could power a magnetic field in the star. Calculations indicate that this mechanism probably cannot account for the existence of high-field magnetic

white dwarfs, but could give rise to a population of low-field magnetic white dwarfs, strongly correlated with the solidification process and modulated by the distribution of the rotation velocities of white dwarfs. Obviously, this mechanism is compatible with the other ones that have been already proposed up to now and could help to solve the present puzzle. Furthermore, if it was really responsible of the existence of part of the magnetic white dwarfs, not only would provide insight to the properties of the Coulomb plasma, but new scenarios to test the theories about the geodynamo mechanism.

References

Althaus, L. G., Córsico, A. H., Isern, J., & García-Berro, E. 2010, A&A Rev., 18, 471
Barrat, J. L., Hansen, J. P. & Mochkovitch, R. 1988, A&A, 199, L15
Christensen, U. R. 2010, Space Sci. Rev., 152, 565
Christensen, U. R., Holzwarth, V., & Reiners, A. 2009, Nat, 457, 167
Ferrario, L., de Martino, D., & Gänsicke, B. T. 2015, Space Sci. Rev., 191, 111
García-Berro, E., Torres, S., Altahus, L. G. et al. 2010, Nat, 465, 194
Giammichele, N., Bergeron, P., Dufour, P. 2012, ApJS, 199, 29
Hollands, M. A., Gansicke, B. T., Koester, D. 2015, MNRAS, 450, 681
Horowitz, C. J., Schneider, A. S., & Berry, D. K. 2010, Phys.Rev.Lett, 104, 231101
Ichimaru, S., Iyetomi, H., & Ogata, S. 1988, ApJ, 334, L17
Isern, J., García-Berro, E., Hernanz, M., & Chabrier, G. 2000, ApJ, 528, 397
Isern, J., Hernanz, M., Mochkovitch, R., & García-Berro, E. 1991, A&A, 241, L29
Isern, J., Mochkovitch, R., García-Berro, E., & Hernanz, M. 1997, ApJ, 485, 308
Kawka, A., Vennes, S., Schmidt, G. O., et al. 2007, ApJ, 654, 499
Kepler, S. O., Pelisoli, I., Jordan, S. et al. 2013, MNRAS, 429, 2934
Mochkovitch, R. 1983, A&A, 122, 212
Nandkumar, R., & Pethick, C. J. 1984, MNRAS, 209, 511
Ogata, S., Iyetomi, H., Ichimaru, S., & Van Horn, H. M. 1993, Phys. Rev. E, 48, 1344
Salaris, M., Cassisi, S., Pietrinferni, A., Kowalski, P. M., & Isern, J. 2010, ApJ, 716, 1241
Schatzman, E. 1958, White Dwarfs (Amsterdam: North Holland Publishing Company)
Schatzman, E. 1982, JPL Proceedings 2d International Coll. of Drps and Bubbles, ed. D. H. Lecroissette, 222
Segretain, L., & Chabrier, G. 1993, A&A, 271, L13
Segretain, L., Chabrier, G., Hernanz, M. et al. 1994, ApJ, 434, 641
Shaviv, G., & Kovetz, A. 1976, A&A, 51, 383
Stevenson, D. J. 1980, Jour. de Physique, 41, C61
Tremblay, P.-E., Bergeron, P., & Gianninas, A. 2011, ApJ, 730, 128
Van Horn H. M. 1968, ApJ, 151, 227
Xu, Z. W. & Van Horn, H. M. 1992, ApJ, 387, 662